RESEARCH PAPER

The Effect of Lanthanum Substitution on the Ferroelectric and Piezoelectric Properties of $(Pb_{0.88}Sr_{0.12})(Zr_{0.54}Ti_{0.44}Sb_{0.02})O_3$ Ceramics

Hossein Goudarzi[1], Saeid Baghshahi[1,*], Reza Tabarzadi[2]

* *baghshahi@eng.ikiu.ac.ir*

[1] Department of Materials Science and Engineering, School of Engineering, Imam Khomeini International University, Qazvin, Iran

[2] Department of Ceramic Engineering, Material and Energy Research Centre, Alborz, Iran

Received: November 2025 **Revised: May 2026** **Accepted: June 2026**

DOI: 10.22068/ijmse.4465

Abstract: *Piezoelectric ceramics based on lead zirconate titanate (PZT) with a composition of $(Pb_{0.88-3x/2}Sr_{0.12}La_x)(Zr_{0.54}Ti_{0.44}Sb_{0.02})O_3$, where x= 0.0, 0.005, and 0.01 were synthesized using conventional solid-state sintering at 1280°C. The effect of lanthanum substitution on the microstructure, ferroelectric, and piezoelectric properties of the samples was studied. The results showed that lanthanum substitution was beneficial for densification of the samples during sintering, and the samples with 1.0 mol% lanthanum exhibited the maximum density of 7340 Kg.m^{-3} when sintered at 1280°C. Moreover, the piezoelectric coefficient (d_{33}), relative dielectric constant (ε_r), dielectric loss (tanδ), electromechanical coupling coefficient (k_p), and the Curie temperature (T_C) of the samples reached the optimal values of 635 pC/N, 3000, 0.018, 0.67, and 195°C, respectively, at 0.5 mol% lanthanum substitution. Furthermore, the bulk density (ρ) was 7310 Kg.m^{-3} for the same sample. The results indicate that the lanthanum-doped PSZTS ceramics can be used in applications such as pulsed transmitting transducers, high sensitivity receivers, and actuators with large displacements.*

Keywords: *PSZTS, Lanthanum additive, Ferroelectric and piezoelectric properties.*

1. INTRODUCTION

By carefully selecting dopant species, the electrical and electromechanical characteristics of PZT ceramics can be engineered. The incorporation of donor or acceptor ions produces compositions generally described as soft or hard PZT [1–3]. Such materials have gained significant technological relevance and are extensively applied in sensing, actuation, and transduction technologies [4, 5].

The remarkable ferroelectric and piezoelectric behavior of PZT ceramics arises primarily when the composition is located near the morphotropic phase boundary (MPB) of the perovskite-type ABO_3 structure. At ambient temperature, this boundary is typically associated with a Zr/Ti ratio of about 52:48. For this reason, many commercially developed ferroelectric ceramics are formulated in the MPB region and are further modified through selective doping to enhance their functional characteristics [2, 3]. A common strategy involves the partial substitution of Pb^{2+} with alkaline-earth ions such as Sr^{2+}, Ca^{2+}, or Ba^{2+} [6, 7]. According to Zheng et al. [7], the incorporation of Sr can lead to superior dielectric and piezoelectric responses compared with undoped PZT. Moreover, the presence of Sr at the A-site shifts the MPB composition toward the tetragonal phase field, where the piezoelectric coefficient can be effectively maximized near—but not precisely at—the MPB.

Reducing the sintering temperature of PZT ceramics while maintaining their ferroelectric and piezoelectric performance has been an important objective in materials research over recent decades. One of the most effective strategies for achieving this goal is the incorporation of suitable dopants that facilitate densification and improve functional properties. Donor dopants, including Nb^{5+} [8, 9], W^{6+} [10], Sb^{5+} [11], and La^{3+} [12–14], have been extensively studied because of their ability to alter defect chemistry and influence domain dynamics in PZT systems.

Among these, Nb-based modifications have also been reported in our previous study [8], which provides a relevant comparison framework for understanding donor-doping effects in similar PZT-based systems. Up to now, however, research on the La-doped $(Pb_{0.88}Sr_{0.12})(Zr_{0.54}Ti_{0.44}Sb_{0.02})O_3$ (PSZTS) ceramics adapted from Zheng et al. [7] has rarely been reported.

In this study, La^{3+} substitution introduces two important effects: (i) a "volume effect" arising from the ionic size mismatch between La^{3+} and Pb^{2+}, leading to slight lattice contraction and structural modification, and (ii) a "charge effect" associated with aliovalent substitution, which induces Pb

[DOI: 10.22068/ijmse.4465]

vacancies for charge compensation and influences densification and electrical properties.

2. EXPERIMENTAL PROCEDURES

Ceramic compositions with the nominal formula $(Pb_{0.88-3x/2}Sr_{0.12}La_x)(Zr_{0.54}Ti_{0.44}Sb_{0.02})O_3$, where x= 0, 0.5, 1.0 mol%, were prepared via a conventional mixed-oxide solid-state reaction technique. High-purity oxide powders were selected as starting materials and weighed according to the required stoichiometry. Homogenization of the powder mixtures was achieved using planetary ball milling in a zirconia container (250 cm^3) with zirconia milling media (15 mm diameter). Milling was conducted at 300 rpm for 20 min with a ball-to-powder mass ratio of 15:1, while distilled water was used as the dispersion medium to ensure uniform mixing. Each batch contained approximately 40 g of powder. After drying, the blended powders were thermally treated at 850°C for 2 h to promote solid-state reactions and phase formation. Controlled heating (2°C min^{-1}) and cooling (5°C min^{-1}) rates were employed to ensure thermal stability. To improve powder homogeneity and minimize agglomeration, the calcined products were subjected to a secondary milling step under identical conditions. For shaping, the powders were granulated using polyvinyl alcohol (PVA) as a temporary binder and compacted into disk-shaped pellets (30 mm diameter, ~4 mm thickness) by uniaxial pressing at 150 MPa. The binder was eliminated through a thermal treatment at 550°C for 3 h. Densification was subsequently carried out at 1280°C for 1 h in sealed alumina crucibles. The heating and cooling schedules during sintering were fixed at 3°C min^{-1} and 5°C min^{-1}, respectively. To suppress lead oxide volatilization at elevated temperature, $PbZrO_3$ powder was placed inside the crucible to provide a PbO-rich atmosphere.

Following sintering, the pellets were mechanically ground and polished to a final thickness of approximately 3 mm. Silver electrodes were formed on both surfaces by applying and firing conductive silver paste. Electrical poling was performed in a silicone oil bath at 120°C under a DC electric field of 2 kV mm^{-1} for 20 min to align ferroelectric domains.

The bulk density of the sintered specimens was evaluated using Archimedes' principle in water. Phase analysis was conducted by X-ray diffraction (PANalytical X'Pert Pro MPD), while microstructural features were examined by field-emission scanning electron microscopy (TESCAN MIRA3 LMU). Dielectric measurements were performed at room temperature at 1 kHz using an impedance-gain analyzer (HP4194A). The dielectric constant was calculated from capacitance data considering specimen geometry and the vacuum permittivity (ε_0= 8.854×10^{-12} $F.m^{-1}$).

The piezoelectric charge coefficient d_{33} was determined with a d_{33} meter (KCF-3500, 110 Hz), and the planar electromechanical coupling factor k_p was obtained using an impedance analyzer (PV520A).

3. RESULTS AND DISCUSSION

3.1. Sintering Behavior

Grain refinement in ceramic systems can occur when dopant ions substitute either A-site or B-site lattice positions. Such substitutions tend to restrict grain growth, an effect commonly linked to the segregation of dopant atoms in the vicinity of grain boundaries. During the densification process, mass transport is predominantly governed by volume diffusion, which is strongly influenced by the number of lattice vacancies present in the structure [15].

The La ions will substitute the Pb ions on the A site of the perovskite structure. Then, to conserve the electron neutrality, Pb vacancies are created, which enhances the volume diffusion and consequently the final densities.

Fig. 1 shows the change of bulk density as a function of lanthanum content for the temperature investigated. As observed, the density of the samples sintered at 1280°C increased with lanthanum content, with the maximum values obtained at 1.0 mol% lanthanum. The optimum density of about 7340 $Kg.m^{-3}$ was recorded for PSZTS ceramics doping with 1.0 mol% lanthanum at the sintering temperature of 1280°C.

The results demonstrate that lanthanum incorporation facilitates the densification process and enables PSZTS ceramics to be sintered at lower temperatures. This improvement can be attributed to variations in vacancy concentration, since lattice vacancies strongly influence the rate of volume diffusion during densification. In equilibrium conditions, pure materials inherently contain a limited number of Pb vacancies. However, the presence of impurities from starting powders or contamination during powder processing may raise the overall equilibrium vacancy concentration within the lattice.

[DOI: 10.22068/ijmse.4465]

In undoped PSZTS ceramics, the naturally existing Pb vacancies are sufficient to sustain an effective densification mechanism, producing a bulk density of 7300 kg·m^{-3} [16]. The incorporation of La^{3+} alters the defect chemistry of the lattice, and to preserve electrical neutrality, additional Pb vacancies are formed. This higher vacancy concentration promotes volume diffusion during sintering, thereby enhancing densification and increasing the final bulk density to approximately 7340 kg·m^{-3} (Fig. 1).

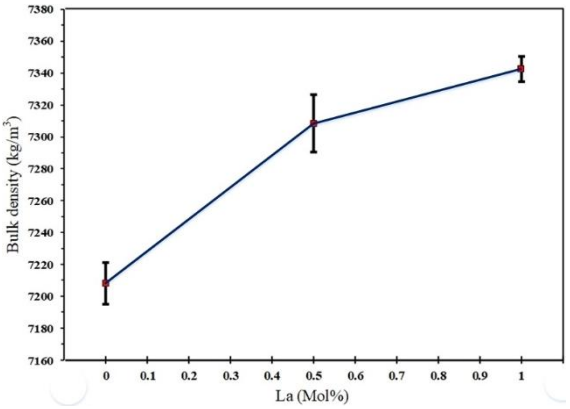

Fig. 1. The variation of bulk density with lanthanum content at 1280°C

3.2. Phase and Microstructure Analysis

Figure 2 displays the X-ray diffraction profiles of $(Pb_{0.88-3x/2}Sr_{0.12}La_x)(Zr_{0.54}Ti_{0.44}Sb_{0.02})O_3$ ceramics prepared with different La contents. Analysis of the diffraction peaks confirms the development of a single-phase perovskite structure. Moreover, the diffraction features indicate the coexistence of tetragonal and rhombohedral crystal phases in both undoped and La-modified PSZTS samples. These findings are consistent with previously published studies [17, 18].

Based on previous studies [18], the crystal structure should consist of a mixture of tetragonal and rhombohedral phases. As the lanthanum content increases up to 1 mol%, the tetragonal phase still dominates over the rhombohedral phase.

The La sites are also considered as donors, whereas Pb vacancies behave as acceptors. The La-Pb pairs can also be considered as dipoles, giving rise to dipolar polarization. As the La content increases, the diffraction peak positions gradually shift toward smaller angles.

The gradual shift of the diffraction peaks with increasing La content can be attributed to changes in the lattice geometry caused by A-site substitution. Specifically, the incorporation of La^{3+} (ionic radius= 1.36 Å) in place of Pb^{2+} (1.49 Å) [19] introduces a smaller cation into the perovskite framework. This size difference promotes a slight contraction of the crystal lattice, which manifests as variations in the lattice parameters and corresponding peak displacement in the XRD patterns.

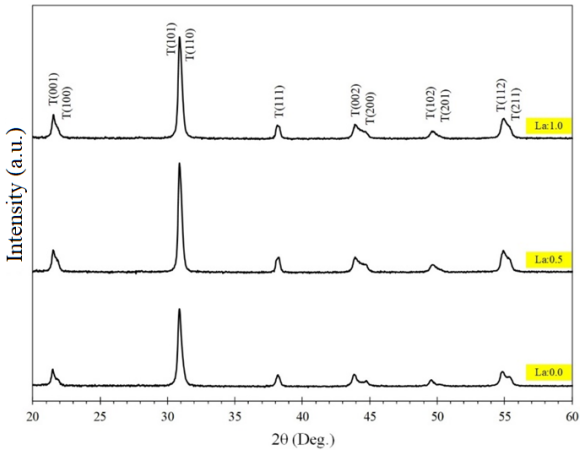

Fig. 2. The XRD patterns of the specimens sintered at 1280°C of $(Pb_{0.88-3x/2}Sr_{0.12}La_x)(Zr_{0.54}Ti_{0.44}Sb_{0.02})O_3$ with different x values

In addition, due to the valence difference between La^{3+} and Pb^{2+}, charge compensation occurs via the formation of lead vacancies, which affects the local lattice distortion and structural stability. Consequently, the slight shift in peak positions indicates a minor modification of the crystal lattice, consistent with compositional variation.

The X-ray diffraction (XRD) results for the samples containing 0, 0.5, and 1 mol% La are summarized in Table 1. All diffraction peaks can be indexed to a tetragonal perovskite structure with P4mm symmetry, corresponding to the reflections (001)/(100), (101)/(110), (111), (002), (200), (102), and (112). No secondary phases are detected, confirming the formation of a single-phase perovskite structure. The strongest diffraction peak is observed for the (101)/(110) plane, which is typical for tetragonal PZT-based ceramics. A slight shift of the diffraction peaks toward higher 2θ values is observed with increasing La content, indicating a small change in the lattice parameters. This shift can be attributed to the substitution of La^{3+} ions for Pb^{2+} ions at the A-site of the perovskite lattice. The calculated lattice parameters show a slight decrease in the c parameter with La doping, while the parameter changes only marginally. Consequently, the tetragonality ratio (c/a) decreases from 1.0138 for the undoped sample to 1.0106 for the sample containing 1 mol%

[DOI: 10.22068/ijmse.4465]

La, suggesting a reduction in tetragonal distortion. The theoretical density (Table 1) shows a slight variation with La addition, changing from 7840 Kg/m³ for x= 0 to 7790 Kg/m³ for x= 0.5 mol% and 7820 Kg/m³ for x= 1 mol%. These changes are mainly related to the small variation in unit cell volume and the decrease in formula weight due to the partial substitution of Pb by La. Overall, La incorporation slightly modifies the lattice parameters while maintaining the single-phase tetragonal perovskite structure.

Lanthanum addition plays a critical role in tailoring the microstructure of PSZTS ceramics. FESEM observations of fractured surfaces (Fig. 3(a–c)) for samples sintered at 1280°C reveal that the specimen with 1.0 mol% La^{3+} achieves the highest degree of densification, in good agreement with bulk density measurements. The enhancement in densification can be rationalized by considering the donor substitution of La^{3+} at the A-site, which necessitates the formation of Pb vacancies to preserve electrical neutrality. XPS findings [20] further support this defect mechanism. The increased vacancy concentration promotes volume diffusion during sintering, thereby accelerating densification. Additionally, La incorporation results in noticeable grain refinement. The reduced grain size is associated with modifications in defect chemistry that alter grain boundary mobility and grain growth kinetics. A quantitative evaluation of grain size distribution was performed using Clemex Vision software, and the calculated distribution parameters are summarized in Table 2.

The incorporation of lanthanum leads to a noticeable reduction in both the average grain size and its standard deviation compared with the La-free ceramics. Grain refinement induced by dopant addition is a common phenomenon in perovskite systems when foreign ions substitute either the A-site or B-site cations. Such substitutions modify the defect chemistry of the lattice and influence the kinetics of grain boundary migration.

Table 1. Summarizes the X-ray diffraction (XRD) parameters, lattice constants, and the calculated theoretical density of the $(Pb_{0.87}Sr_{0.12}La_x)(Zr_{0.54}Ti_{0.44}Sb_{0.02})O_3$ ceramics compositions

mole%	Pos. [°2 Th.]	(hkl)	Rel. Int. [%]	a	c	c/a	$\rho_{theoretical}$ (Kg/m^3)
0.0	21.57729	T (001) (100)	12.99	4.035	4.091	1.0139	7840
	30.92431	T (101) (110)	100.00				
	37.74680	T (111)	13.75				
	43.55266	T (002)	11.09				
	44.2183	T (200)	3.77				
	49.70169	T (102)	6.36				
	54.54230	T (112)	19.68				
0.5	21.59699	T (001) (100)	15.5	4.041	4.088	1.0116	7790
	30.94329	T (101) (110)	100.00				
	37.95745	T (111)	16.95				
	43.75266	T (002)	12.54				
	44.4067	T (200)	4.56				
	49.72173	T (102)	8.65				
	54.74486	T (112)	22.29				
1.0	21.627310	T (001) (100)	13.99	4.038	4.080	1.104	7820
	30.974310	T (101) (110)	100.00				
	38.257450	T (111)	14.75				
	44.052660	T (002)	13.09				
	44.706700	T (200)	4.06				
	49.750740	T (102)	7.05				
	55.044860	T (112)	21.17				

Table 2. Distribution parameters of the grain size for the different ceramics

La	Minimum	Maximum	Average	Standard
mol%	(µm)	(µm)	(µm)	deviation
0.0	1.26	5.20	2.73	1.02
0.5	0.49	5.48	2.10	0.77
1.0	0.66	3.38	1.61	0.49

[DOI: 10.22068/ijmse.4465]

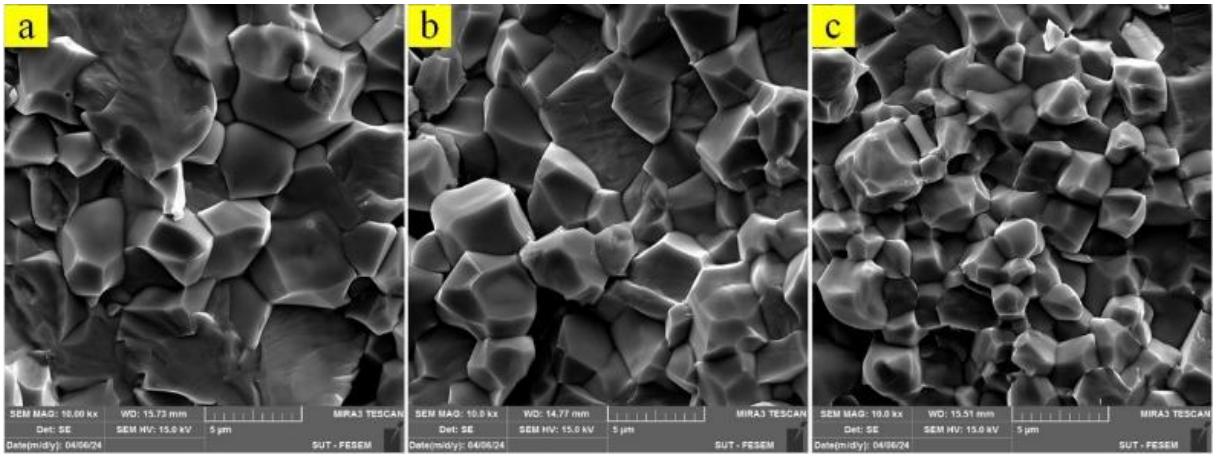

Fig. 3. The FESEM photomicrographs of the fractured surfaces of the specimens sintered at 1280°C, a) 0.0, b) 0.5 and c) 1.0 mole% La

The reduction in grain size is frequently explained by the inhibition of grain growth through a boundary-pinning mechanism. In this model, dopant species or associated defects tend to segregate near grain boundaries and decrease their mobility, thereby limiting grain coarsening during sintering. However, as discussed by Hammer and Hoffmann [15], direct experimental verification of this pinning mechanism remains limited, and alternative explanations such as solute drag effects or changes in diffusion behavior may also contribute to the observed grain growth suppression.

3.3. The Dielectric and Piezoelectric Properties

Figure 4(a,b) shows the variation of dielectric loss and relative dielectric constant for samples sintered at 1280°C. The results indicate that increasing the lanthanum content generally leads to an enhancement of the dielectric constant as well as changes in the loss factor (tanδ). The improvement in dielectric properties is closely related to densification behavior. Higher density reduces the pore volume within the ceramic matrix, which typically increases the dielectric constant while lowering dielectric loss. The composition doped with 1.0 mol% La exhibits the highest dielectric constant together with the lowest dielectric loss, consistent with its maximum densification.

In addition, the larger dielectric constant observed in La-modified samples compared with the undoped ceramic may be associated with increased domain wall mobility caused by a higher concentration of Pb vacancies introduced through donor doping [15]. The observed enhancement in domain wall motion is attributed to donor doping (La^{3+} and Sb^{5+}), which induces Pb vacancies for charge compensation. Unlike oxygen vacancies in acceptor-doped (hard) systems that strongly pin domain walls, Pb vacancies in donor-doped (soft) PZT systems result in reduced pinning and enhanced domain wall mobility.

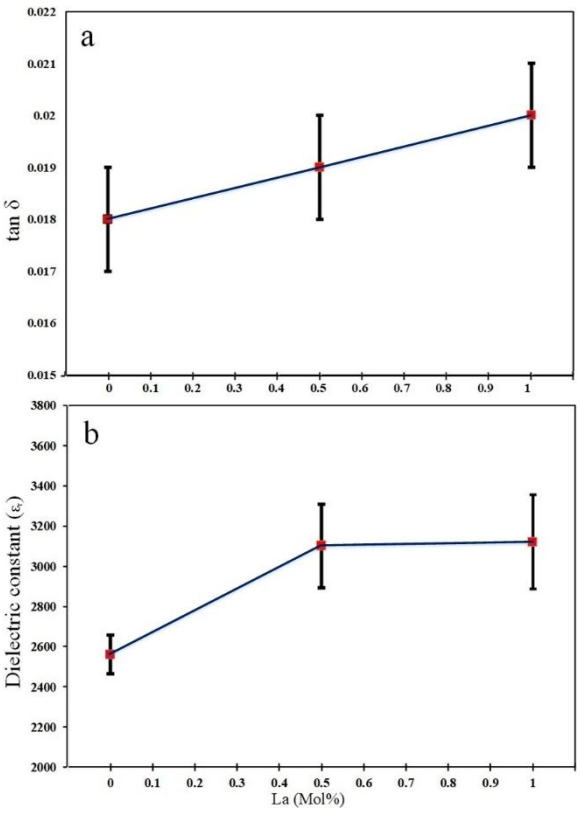

Fig. 4. Illustrates the dependence of a) dielectric loss (tanδ) and b) relative dielectric constant with lanthanum content at 1280°C

Figures 5 and 6 show the piezoelectric coefficient d_{33} and the planar electromechanical coupling coefficient k_p for the samples sintered at 1280°C.

[DOI: 10.22068/ijmse.4465]

As observed, with increasing La content, the piezoelectric coefficient d_{33} and the planar electromechanical coupling k_p of the La-doped PSZTS ceramics increased greatly, reaching the maxima at 0.5 mol% La.

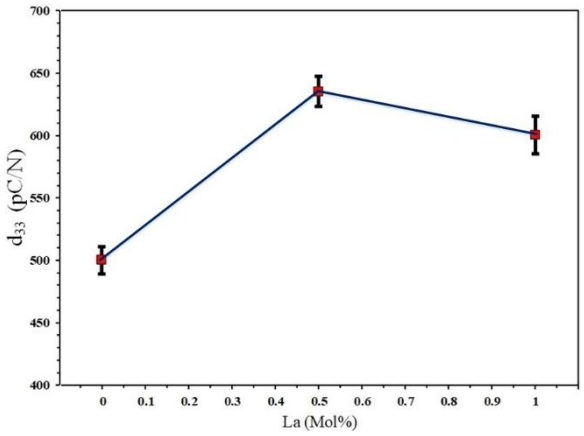

Fig. 5. The changes in the charge coefficient (d_{33}) with lanthanum content at 1280°C

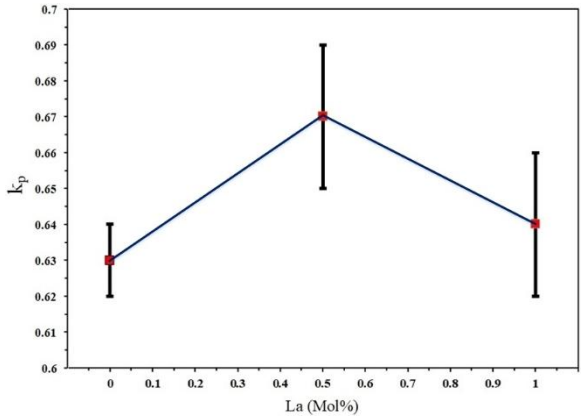

Fig. 6. The variation of the planar electromechanical coupling coefficient (k_p) with lanthanum content at 1280°C

The addition of lanthanum plays an important role in tailoring the functional properties of PZT-based ceramics, including their dielectric, ferroelectric, and piezoelectric responses [1]. La_2O_3 behaves as a donor dopant and substitutes for Pb^{2+} at the A-site of the perovskite lattice. Because of the valence mismatch between La^{3+} and Pb^{2+}, charge compensation occurs through the formation of Pb vacancies. The presence of these vacancies facilitates the movement of ferroelectric domain walls, reduces internal lattice stresses, and consequently enhances the piezoelectric coefficients d_{33} and k_p [15]. However, excessive lanthanum incorporation can be detrimental. At higher concentrations, surplus La^{3+} ions tend to segregate at grain boundaries, which restricts domain wall switching during polarization and leads to a reduction in piezoelectric performance [15].

The optimum properties in the present study were observed at a lanthanum content of 0.5 mol%, yielding a maximum d_{33} value of 635 pC/N and a coupling coefficient k_p of 0.67.

Figure 7a (0 mol% La), b (0.5 mol% La), and c (1.0 mol% La) show the variation of relative permittivity with temperature for samples sintered at 1280°C, measured at three frequencies: 1 kHz, 10 kHz, and 100 kHz. The Curie temperature (Tc) decreases from approximately 230°C for the undoped sample (0 mol% La^{3+}) to about 185°C for the sample containing 1.0 mol% La^{3+}. In addition to lowering Tc, the substitution of La^{3+} broadens the phase transition peak. Furthermore, the εr–T curves exhibit no significant shift with increasing frequency.

Table 3 compares the dielectric and piezoelectric properties of PSZTS ceramics with different dopants. In the present work, lanthanum substitution leads to improved electromechanical performance, with the optimum values obtained at 0.5 mol% La. Further increase in La content results in a decrease in d_{33}, k_p, and T_C, indicating that excessive La substitution is detrimental to the overall performance.

Table 3. Comparison of the dielectric and piezoelectric properties of PSZTS ceramics doped with various elements and different La concentrations

Dopant in PSZTS	Sintering Temperature (°C)	ε_r (at 1 kHz)	d_{33} pC/N	k_p	Ref.
$Pb_{0.875}Sr_{0.125}(Zr_{0.54}Ti_{0.46})O_3$	1280	1237	~240	47	[6]
$Pb_{0.875}Sr_{0.125}(Zr_{0.53}Ti_{0.47})O_3$	1280	1325	~285	51	[6]
$Pb_{0.88}Sr_{0.12}(Zr_{0.54}Ti_{0.44}Sb_{0.02})O_3$	1250	2400	527	-	[21]
$Pb_{0.88}Sr_{0.12}(Zr_{0.54}Ti_{0.44}Sb_{0.02})O_3$	1170	~2000	~600	-	[22]
$Pb_{0.88}Sr_{0.12}(Zr_{0.54}Ti_{0.44}Sb_{0.02})O_3$	1250	1479	339	66	[23]
$Pb_{0.88}Sr_{0.12}(Zr_{0.54}Ti_{0.44}Sb_{0.02})O_3$	1280	2560±96	500±11	63±1	Present paper
$Pb_{0.875}Sr_{0.12}La_{0.005}(Zr_{0.54}Ti_{0.44}Sb_{0.02})O_3$	1280	3000±209	635±12	67±2	Present paper
$Pb_{0.875}Sr_{0.12}La_{0.010}(Zr_{0.54}Ti_{0.44}Sb_{0.02})O_3$	1280	3120±236	600±15	64±2	Present paper

[DOI: 10.22068/ijmse.4465]

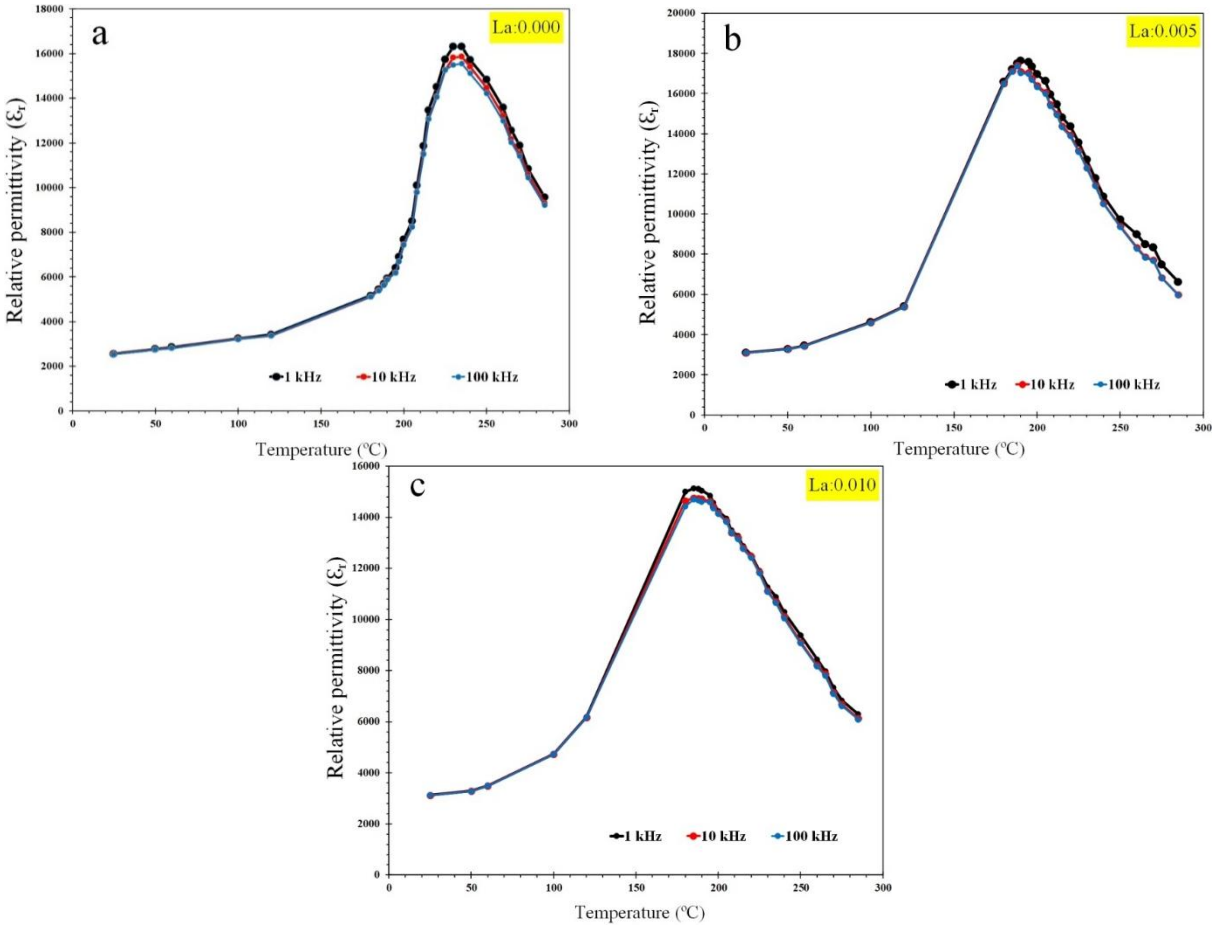

Fig. 7. Temperature dependence of the relative permittivity (ε_r) for, a) $(Pb_{0.88}Sr_{0.12})(Zr_{0.54}Ti_{0.44}Sb_{0.02})O_3$ and b) $(Pb_{0.875}Sr_{0.12}La_{0.005})(Zr_{0.54}Ti_{0.44}Sb_{0.02})O_3$, c) $(Pb_{0.87}Sr_{0.12}La_{0.01})(Zr_{0.54}Ti_{0.44}Sb_{0.02})O_3$ ceramics, various frequencies, showing the Curie temperature

The results show that the incorporation of the lanthanum to the perovskite structure promotes the Pb vacancies (A site) and may likely have an intense effect on the domain motions, because of the expansion in the unit cell in the direction of the polarization [19]. The increase of the lanthanum concentration increases the A-site vacancies concentration and a higher ferroelectric domain motion [1, 16].

La substitution (>0.5 mol %) was decrease in the piezoelectric charge coefficients (d_{33}) (Fig. 5), the planar electromechanical coupling coefficient (k_p) (Fig. 6).

The incorporation of lanthanum into the perovskite lattice facilitates the formation of Pb vacancies at the A-site, which play an important role in governing ferroelectric domain behavior. These vacancies can enhance domain wall mobility, potentially due to lattice expansion along the polarization direction [19]. Consequently, increasing the La concentration leads to a higher concentration of A-site vacancies and greater domain wall activity [1, 16].

However, excessive La substitution (>0.5 mol%) results in a deterioration of the piezoelectric properties, as reflected by the reduction in the piezoelectric charge coefficient d_{33} (Fig. 5) and the planar electromechanical coupling coefficient k_p (Fig. 6).

4. CONCLUSIONS

A significant improvement in the piezoelectric properties of $(Pb_{0.88}Sr_{0.12})(Zr_{0.54}Ti_{0.44}Sb_{0.02})O_3$ samples doped with La^{3+} was achieved. Grain size decreased with the increase of La substitution, where the highest grain size was observed in the La free composition.

Lanthanum doping resulted in a substantial improvement in the piezoelectric properties of $(Pb_{0.88}Sr_{0.12})(Zr_{0.54}Ti_{0.44}Sb_{0.02})O_3$ ceramics. A progressive reduction in grain size was observed with increasing La content, while the undoped

[DOI: 10.22068/ijmse.4465]

composition exhibited the largest grain size. In addition, lanthanum substitution significantly enhanced densification and allowed the PSZTS ceramics to be sintered effectively at lower temperatures. The sample containing 1.0 mol% La^{3+} achieved the highest density and the lowest dielectric loss at a sintering temperature of 1280°C. Nevertheless, the optimum dielectric and piezoelectric performance was obtained for the composition with 0.5 mol% La^{3+}. The best values of d_{33}, ε_r, $\tan\delta$, k_p, ρ and T_C of the samples reached the optimal values of 635 pC/N, 3000, 0.018, 0.67 and 195°C, respectively at 0.5 mol% lanthanum substitution, which are promising for pulsed transmitting transducers, high sensitivity receivers and actuators with large displacements.

REFERENCES

[1] Jaffe, B., Cook, W.R., Jaffe, H., Piezoelectric Ceramics. Academic Press, New York, 1971.

[2] Haertling, G.H., "Ferroelectric Ceramics: History and Technology", J. Am. Ceram. Soc., 1999, 82, 797-818.

[3] Takahashi, S., "Effects of impurity doping in lead zirconate titanate ceramics", Ferroelectrics, 1982, 41, 143-156.

[4] Moulson A.J., Herbert, J.M., Electroceramics: Materials, Properties, Applications, Chapman and Hall, New York, 1990.

[5] Uchino, K., Ferroelectric Devices, Marcel Dekker, New York, 2000.

[6] Kulcsar, F., "Electromechanical Properties of Lead Titanate Zirconate Ceramics with Lead Partially Replaced by Calcium or Strontium", J. Am. Ceram. Soc. 1959, 42, 343-349.

[7] Zheng, H., Reaney, I. M., Lee, W. E., Jones, N., Thomas, H., "Effects of Strontium Substitution in Nb-Doped PZT Ceramics", J. Eur. Ceram. Soc., 2001, 21, 1371–1375.

[8] Goudarzi H., Baghshahi, S., "PZT ceramics prepared through a combined method of B-site precursor and wet mechanically activated calcinate in a planetary ball mill", Ceram. Int., 2017, 43, 3873–3878.

[9] Chu, S.Y., Chen, T.Y., Tsai I.T., Water, W. "Doping effects of Nb additives on the piezoelectric and dielectric properties of PZT ceramics and its application on SAW device", Sensor Actuators, A. 2004, 133, 198-203.

[10] Zong, X.M., Yang, Z.P., Li H., Yuan, M.B. "Effects of WO_3 addition on the structure and electrical properties of Pb_3O_4 modified PZT–PFW–PMN piezoelectric ceramics", Mater. Res. Bull., 2006, 41, 1447-54.

[11] Zhou, T. "The effect of doping Sb_20_3 in high d_{33}, g_{33} PZT Piezoelectric Ceramics", Ferroelectrics, 1997, 195, 101-104.

[12] Kalem, V., Cam I., Timucin, M., "Dielectric and piezoelectric properties of PZT ceramics doped with strontium and lanthanum", Ceram. Int., 2001, 37, 1265–1275.

[13] Singh, V., Kumar, H.H., Kharat, D.K., Hait S., Kulkarni, M.P., "Effect of Lanthanum substitution on ferroelectric properties of Niobium doped PZT ceramics", Mater. Lett., 2006, 60, 2964-68.

[14] Laurent, M. Schreiner, U., Langjahr, P.A., Glazounov A.E., Hoffmann, M.J., "Micro-structural and electrical characterization of La-doped PZT ceramics prepared by a precursor route", J. Eur. Ceram. Soc., 2001, 21, 1495-98.

[15] Hammer M., Hoffmann, M.J., "Sintering model for mixed-oxide-derived lead zirconate titanate ceramics", J. Am. Ceram. Soc., 1998, 81, 3277-3284.

[16] Gerson, R., "Variation in ferroelectric characteristics of lead zirconate titanate ceramics due to minor chemical modifications", J. Appl. Phys. 31, 1960, 188-194.

[17] Zheng, H., Ph.D. Thesis, Structure-property relations in Sr, Nb, Ba doped lead zirconate titanate, University of Sheffield, 2001.

[18] Kalem, V., Ph.D. Thesis, Development of Piezoelectric Ceramics for Ultrasonic Motor Applications, Middle East Technical University, 2011.

[19] Shannon R. D., Prewitt, C. T., "Effective ionic radii in oxides and fluorides", Acta Cryst., 1970, B26, 1046.

[20] Goudarzi, H., Baghshahi, S., Tabarzadi, R., "Comparison of Dielectric and Piezo-electric Properties of Sb- and Nb-Doped $Pb_{0.87}Sr_{0.12}La_{0.01}(Zr_{0.54}Ti_{0.44}X_{0.02})O_3$ Ceramics", Ceram. Int., 2026, In press, https://doi.org/10.1016/j.ceramint.2026.05.071.

[21] Eitssayeam, S., Jarupoom P., Rujijanagul, G. "High Dielectric and Piezoelectric Properties Observed in Annealed $Pb_{0.88}Sr_{0.12}Zr_{0.54}Ti_{0.44}Sb_{0.02}O_3$ Ceramics", Ferroelectrics, 2013, 451, 48–53.

[22] Zheng, H., Reaney, I. M., Lee, W. E., Jones, N. Thomas, H., "Surface Decomposition of

[DOI: 10.22068/ijmse.4465]

Strontium-Doped Soft $PbZrO_3$–$PbTiO_3$", J. Am. Ceram. Soc., 2002, 85, 207–212.

[23] Jaita, P., Kruea-In, C., Rujijanagul, G. "Influence of Al_2O_3 Nanoparticles Incorporation on the Structure and Electrical Properties of $Pb_{0.88}Sr_{0.12}Zr_{0.54}Ti_{0.44}Sb_{0.02}O_3$ Ceramics", Nanomaterials and Nanotechnology, 2016, 6, 1-7.

[DOI: 10.22068/ijmse.4465]